MCB
Journals.ASM.org

A Critical Role for the Wnt Effector Tcf4 in Adult Intestinal Homeostatic Self-Renewal

Johan H. van Es,[a] Andrea Haegebarth,[a]* Pekka Kujala,[a,b] Shalev Itzkovitz,[c] Bon-Kyoung Koo,[a] Sylvia F. Boj,[a] Jeroen Korving,[a] Maaike van den Born,[a] Alexander van Oudenaarden,[c] Sylvie Robine,[d] and Hans Clevers[a]

Hubrecht Institute for Developmental Biology and Stem Cell Research & University Medical Centre Utrecht, Utrecht, Netherlands[a], Antoni van Leeuwenhoek Hospital/Netherlands Cancer Institute, Amsterdam, Netherlands[b]; Department of Physics & Biology, Massachusetts Institute of Technology, Cambridge Massachusetts, USA[c]; and Morphogenesis and Intracellular Signaling, Institut Curie-CNRS, Paris, France[d]

Throughout life, intestinal Lgr5$^+$ stem cells give rise to proliferating transient amplifying cells in crypts, which subsequently differentiate into one of the five main cell types and migrate along the crypt-villus axis. These dynamic processes are coordinated by a relatively small number of evolutionarily conserved signaling pathways, which includes the Wnt signaling pathway. The DNA-binding proteins of the T-cell factor family, Tcf1/Tcf7, Lef, Tcf3/Tcf7l1, and Tcf4/Tcf7l2, constitute the downstream effectors of the Wnt signaling pathway. While Tcf4 is the major member active during embryogenesis, the role of these Wnt effectors in the homeostasis of the adult mouse intestinal epithelium is unresolved. Using *Tcf1*$^{-/-}$, *Tcf3*^{flox}, and novel *Tcf4*^{flox} mice, we demonstrate an essential role for Tcf4 during homeostasis of the adult mouse intestine.

The epithelium of the small intestine and colon represents the fastest self-renewing tissue in mammals. The murine small intestine contains about 1 million invaginations, the crypts of Lieberkühn, which represent the proliferative compartments and are scattered around the base of extrusions, the villi that are covered with differentiated epithelial cells. The colon has crypts but no villi (reviewed in reference 26). Newly produced intestinal epithelial cells derive from Lgr5-expressing multipotent stem cells (2). Each crypt base contains about 14 long-lived stem cells which divide symmetrically every day (12, 40, 42). Recently, it has been proposed that *Bmi1* marks a reserve pool of stem cells residing at position +4 (36, 43). However, by three-color single-molecule fluorescent *in situ* hybridization, *Bmi1* is found to be expressed in all proliferative crypt cells, including the Lgr5$^+$ intestinal stem cells (19). Indeed, *Bmi1*-based lineage tracing can initiate in any cell in the crypt, including in Lgr5 stem cells (43). Randomly, half of the Lgr5$^+$ daughter cells become transit-amplifying (TA) cells which migrate upwards along the crypt-villus axis while dividing 4 to 5 times. The TA cells exit the mitotic cell cycle and differentiate into one of the five main cell types: mucus-secreting goblet cells, hormone-secreting enteroendocrine cells, antimicrobial peptide and Wnt-secreting Paneth cells, hydrolase-secreting enterocytes, and opioid-secreting Tuft cells. Enterocytes, goblet, enteroendocrine, and tuft cells continue migrating up the villus, whereas Paneth cells migrate downwards to reside at the crypt base, where they serve as niche cells to the Lgr5 stem cells (7, 8, 13). Upon reaching the tips of the small intestinal villi, the cells undergo apoptosis and are exfoliated into the lumen.

The structural and functional integrity of the intestine is largely dependent upon a continuous and well-organized flow of the different cell lineages. The morphogenetic process and the acquisition of particular cell fates are coordinated by a relatively small number of highly evolutionarily conserved signaling pathways, including the canonical Wnt signaling pathway (reviewed in references 9 and 50). This pathway has been shown to play a central role in cell proliferation, differentiation, and stem cell maintenance. Wnt signaling controls developmental fates through the regulation of *Tcf/Lef* target genes via the dedicated coactivator of Wnt, β-catenin. In the absence of a Wnt signal, the cytosolic levels of β-catenin are kept low by the destruction complex, which includes axin, adenomatous polyposis coli (APC), and glycogen synthase kinase 3β (GSK3β). This interaction induces phosphorylation of β-catenin, resulting in its ubiquitination and degradation by the proteasome. In the absence of β-catenin, T-cell factor (TCF) is thought to function as a repressor of Wnt target gene expression. Upon Wnt signaling, the activity of the destruction complex is inhibited and β-catenin is no longer degraded and translocates to the nucleus, where it interacts with a member of the TCF family (Tcf1, Lef, Tcf3, and Tcf4) to turn on the Wnt genetic program.

Genetic studies have shown that canonical Wnt signaling plays an essential role in regulating intestinal epithelial cell proliferation. Genetic alterations in APC, β-catenin, or axin lead to the formation of intestinal adenomas as a result of deregulated nuclear accumulation of β-catenin and constitutive activation of Wnt target genes associated with proliferation of epithelial cells (22, 25, 29, 32, 37). Moreover, frameshift mutations or specific gene fusions of Tcf7l2 are implicated in colorectal cancer (3, 17, 41). In neonatal mice lacking *Tcf4*, proliferative crypts do not develop (23). In adult mice, the conditional deletion of β-catenin or the overexpression of the diffusible Wnt inhibitor Dickkopf 1 results in the complete block of cell proliferation (18, 24, 34). Moreover, transgenic expression of R-spondin-1, a Wnt agonist that acts through the Lgr4/5-Wnt receptor complex (10), results

Received 17 September 2011 **Returned for modification** 19 October 2011
Accepted 25 February 2012
Published ahead of print 5 March 2012
Address correspondence to Hans Clevers, h.clevers@hubrecht.eu.
* Present address: Bayer Healthcare AG, Berlin, Germany.
J.H.V.E. and A.H. contributed equally to this article.
Supplemental material for this article may be found at http://mcb.asm.org/.

doi:10.1128/MCB.06288-11

in a massive hyperproliferation of intestinal crypts (21). Simultaneous deletion of Lgr4 and Lgr5, the receptors for R-spondins, leads to the demise of the crypts (10).

The Wnt-driven crypt gene program has been uncovered, and the roles of individual Wnt target genes (including *Ascl2*, *Lgr4/5*, *EphB2/B3*, *frizzled-5*, c-*Myc*, and *Sox9*) have been studied extensively in transgenic mouse models (4, 5, 10, 28, 45, 47). Together, these data provide clear evidence that in addition to proliferation, the control of intestinal stem cell fate, stem cell maintenance, maturation, and sorting of crypt epithelial cells depends on the correct dosing of Wnt signals along the crypt axis.

The expression pattern of the different Tcf proteins during adult gut development and homeostasis has been described previously (16). In the small intestine, *Tcf4* is expressed along the entire crypt-villus axis, while in the colon, *Tcf4* expression is low at the crypt base and high in the noncycling cells in the upper colonic crypt (1, 16). In the adult small intestine, *Tcf1* (itself a Wnt target gene) is expressed at the bottom of the proliferating crypts and is strongly upregulated in intestinal adenomas (16). *Lef* is expressed in intestinal polyps, while in normal epithelium, *Lef* transcripts are absent (16). In adult tissue, *Tcf3* is mainly expressed in the proliferative compartment of colon in a gradient inverse to that of *Tcf4*. Of note, genetic data in other systems imply that *Tcf3* primarily functions as a transcriptional repressor in vertebrate embryos and stem cells (20, 27). The aim of this study was to determine the role of the different members of the Tcf family in adult intestinal tissue homeostasis.

MATERIALS AND METHODS

Generation of floxed *Tcf4* mice. Conditional $Tcf4^{LoxP}$ mice were generated through homologous recombination in embryonic stem (ES) cells, as depicted in Fig. S2 in the supplemental material. Both flanking arms were generated by high-fidelity PCRs from male 129/Ola-derived bacterial artificial chromosome DNA and subsequently cloned into PL451. The targeting construct (100 μg) was linearized and transfected into male 129/Ola-derived IB10 ES cells by electroporation (800 V, 3 F). Recombinant embryonic stem cell clones expressing the neomycin gene were selected in medium supplemented with G418 (250 μg/ml). Approximately 200 recombinant embryonic stem cell clones were screened by Southern blotting. About 10% of the isolated clones showed homologous recombination. Two positive clones were selected and injected into C57BL/6 mouse-derived blastocysts using standard procedures. Both clones gave germ line transmission. The neomycin selection cassette was flanked by Frt recombination sites and excised *in vivo* by crossing the mice with the general FLP deleter strain (Jackson Laboratories). The histological analysis of the intestines of both lines gave completely identical results.

RNA extraction and RT-PCR. RNA extraction on isolated intestinal epithelial cells and reverse transcription (RT) were performed as described previously (33). The primers used for detection of the splice variants are described elsewhere (49).

Generation of compound mice. The transgenic line $Villin^{Creert2}$ was crossed with $Tcf4^{LoxP}$, $Tcf3^{LoxP}$, and/or *Tcf1* mice to obtain strain $Villin^{Creert2}$_$Tcf4^{LoxP/LoxP}$_$Tcf3^{LoxP/LoxP}$_$Tcf1^{hom}$, $Villin^{Creert2}$_$Tcf3$-$^{LoxP/LoxP}$, $Villin^{Creert2}$_$Tcf4^{LoxP/LoxP}$_$Tcf3^{LoxP/LoxP}$, $Villin^{Creert2}$_$Tcf3^{LoxP/LoxP}$_$Tcf1^{hom}$, and $Villin^{Creert2}$_$Tcf4^{LoxP/LoxP}$ mice as well as various genotypic controls. The Cre enzyme was induced by a single intraperitoneal injection on day 0 of 200 μl tamoxifen (5 mg/200 μl; Sigma-Aldrich) dissolved in sunflower oil. The 6- to 12-week-old mice were sacrificed, and the intestines were isolated on different days after *cre* induction. All procedures were performed in compliance with local animal welfare laws, guidelines, and policies.

Immunohistochemistry and *in situ* hybridization. Freshly isolated intestines were flushed with formalin (4% formaldehyde in phosphate-buffered saline [PBS]) and fixed by incubation in a 10-fold excess of formalin overnight (O/N) at room temperature. The formalin was removed, and the intestines were washed twice in PBS at room temperature. The intestines were then transferred to a tissue cassette and dehydrated by serial immersion in 20-fold volumes of 70%, 96%, and 100% ethanol (EtOH) for 2 h each at 4°C. Excess ethanol was removed by incubation in xylene for 1.5 h at room temperature, and the cassettes were then immersed in liquid paraffin (56°C) overnight. Paraffin blocks were prepared using standard methods. Tissue sections of 4 μm were dewaxed by immersion in xylene (2 times, 5 min) and hydrated by serial immersion in 100% EtOH (2 times, 1 min), 96% EtOH (2 times, 1 min), 70% EtOH (2 times, 1 min), and distilled water (2 times, 1 min). Endogenous peroxidase activity was blocked by immersing the slides in peroxidase blocking buffer (0.040 M citric acid, 0.121 M disodium hydrogen phosphate, 0.030 M sodium azide, 1.5% hydrogen peroxide) for 15 min at room temperature. Antigen retrieval was performed (see details below for each antibody), and blocking buffer (1% bovine serum albumin [BSA] in PBS) was added to the slides for 30 min at room temperature. Primary antibodies were then added, and the slides were incubated as detailed below. The slides were then rinsed in PBS, and secondary antibody was added (polymer horseradish peroxidase-labeled anti-mouse or -rabbit antibody; Envision) for 30 min at room temperature. Slides were again washed in PBS, and bound peroxidase was detected by adding diaminobenzidine (DAB) substrate for 10 min at room temperature. Slides were then washed 2 times in PBS, and nuclei were counterstained with Mayer's hematoxylin for 2 min, followed by two rinses in distilled water. Sections were dehydrated by serial immersion for 1 min each in 50% EtOH and 60% EtOH, followed by 2 min each in 70% EtOH, 96% EtOH, 100% EtOH, and xylene. Slides were mounted in Pertex mounting medium, and a coverslip was placed over the tissue section. Antigen retrieval was performed by boiling samples for 20 min in 10 mM sodium citrate buffer (pH 6.0). Antibodies used were mouse anti-Ki67 (1:100 dilution; Novocastra), rabbit antisynaptophysin (1:200 dilution; Dako), rabbit antilysozyme (1:1,750 dilution; Dako), rabbit anti-CD44 (1:200 dilution; firma), rabbit anti-Sox9 (1:600 dilution; Chemicon), rabbit anti-Dcamkl1 (1:200 dilution; Abcam), and mouse anti-Tcf4 (1;250 dilution; Millipore). Incubation of antibodies was performed overnight in BSA in PBS at 4°C for antibodies directed against bromodeoxyuridine, CD44, and Tcf4 and for 1 h at room temperature for antibodies directed against Ki67, synaptophysin, β-catenin, Sox9, and lysozyme. In all cases, reagent from the Envision$^+$ kit (Dako) was used as a secondary reagent. Stainings were developed with DAB. Slides were counterstained with hematoxylin and mounted.

For *in situ* hybridization, 8-μm-thick sections were rehydrated as described above. Afterward, the sections were treated with 0.2 M sodium chloride and proteinase K. Slides were postfixed, and sections were then demethylated with acetic anhydride and prehybridized. Hybridization was done in a humid chamber with 500 ng/ml freshly prepared digoxigenin (DIG)-labeled RNA probe of Olfm4 (image clone 1078130) or cryptdin-1 (image clone 1096215). Sections were incubated for at least 48 h at 68°C. The slides were washed, and incubation of the secondary anti-DIG antibody (Roche) was done at 4°C overnight. The next day, sections were washed and developed using Nitro Blue Tetrazolium chloride–5-bromo-4-chloro-3-indolylphosphate.

Multicolor single-molecule fluorescent *in situ* hybridization. The duodenum was quickly dissected, flushed with cold 4% formaldehyde/paraformaldehyde in PBS, and incubated at 4°C for 2 to 3 h with gentle agitation. Subsequently, the tissue was put into prechilled cryoprotecting solution (4% formaldehyde-paraformaldehyde–30% sucrose–PBS) and incubated overnight at 4°C with gentle agitation. After the O/N incubation, the tissue was put into the molds filled with cold OCT and stored at −80°C. Probe libraries were designed and constructed as described previously (19). Hybridizations were done overnight with two differentially labeled probes using Bmi1-Cy5 and Lgr5-tetramethylrhodamine (TMR) fluorophores. An additional fluorescein isothiocyanate-conjugated antibody for E-cadherin (BD Biosciences) was added to the hybridization mix

and used for protein immunofluorescence to detect cell borders. DAPI (4′,6-diamidino-2-phenylindole) dye for nuclear staining was added during the washes. Images were taken with a Nikon TE2000 inverted fluorescence microscope equipped with a ×100 oil-immersion objective and a Princeton Instruments camera using MetaMorph software (Molecular Devices, Downington, PA). All images are filtered with a Laplacian or Gaussian filter and are maximal projections of 15 stacks spaced 0.3 μm apart in the *z* direction.

Electron microscopic analysis. As described previously (2), a piece of 1.5 cm of the intestine was fixed in Karnovsky's fixative (2% paraformaldehyde, 2.5% glutaraldehyde, 0.1 M sodium cacodylate, 2.5 mM $CaCl_2$, 5 mM $MgCl_2$, pH 7.4) O/N at room temperature (18 to 22°C). The samples were embedded in Epon resin and were examined with a Phillips CM10 microscope.

X-Gal (5-bromo-4-chloro-3-indolyl-β-D-galactopyranoside) staining. To determine the pattern of Cre-mediated recombination of the *Rosa26*^{LacZ} reporter locus in the Villin^{Creert2} mice, the intestines were isolated upon *cre* induction and immediately incubated for 2 h in a 20-fold volume of ice-cold fixative (1% formaldehyde, 0.2% gluteraldehyde, 0.02% NP-40 in phosphate-buffered saline without Ca^{2+} and Mg^{2+} [PBS0]) at 4°C on a rolling platform. Staining for the presence of β-galactosidase (LacZ) activity was performed as described previously (2). The stained tissues were transferred to tissue cassettes, and paraffin blocks were prepared with standard methods. Tissue sections (4 μm) were prepared and counterstained with neutral red.

Organoid culture. Organoids of small intestine were established from freshly isolated crypts. Incubation in PBS (pH 7.4) containing 2 mM EDTA was used for the isolation of the intestinal crypts. The culture conditions of mouse small intestine organoids have been described elsewhere (38). The organoids were grown with standard ENR medium (50 ng/ml mouse epidermal growth factor [EGF], 100 ng/ml noggin, and 500 ng/ml mouse R-spondin-1). Incubation with tamoxifen induced the deletion of *Tcf4* in the organoids derived from the Villin^{Creert2}_Tcf4$^{LoxP/LoxP}$ mice.

RESULTS

***Tcf1* and *Tcf3* are dispensable for adult intestinal homeostasis.** *Tcf1* and *Tcf3* are both expressed in the adult intestine. *Tcf3* homozygous knockout (KO) mice die at about embryonic day 9.5 (E9.5), well before the formation of the intestine (27). To be able to study the consequence of a complete and specific ablation of *Tcf3* in the small and large intestine, we generated Villin^{Creert2}_Tcf3$^{LoxP/LoxP}$ compound mouse (11, 27). Villin^{Creert2} mice express a tamoxifen-inducible version of the Cre enzyme under the control of the villin promoter, which drives stable and homogeneous expression of the Cre recombinase in almost all epithelial cells in the small intestine and, to a lesser extent, of the large intestine (11). The colons and small intestines of adult Villin^{Creert2}_Tcf3$^{LoxP/LoxP}$ mice and their littermate controls were histologically analyzed on different days after *cre* induction (days 1, 3, 7, and 32). Intestinal sections were stained with cell-type-specific reagents to detect the main intestinal cell types and proliferating cells. The Villin^{Creert2}_Tcf3$^{LoxP/LoxP}$ mice exhibited, at all time points, normal numbers of stem, differentiated, and proliferating cells compared to their control littermates. The results of the histological analysis of the small intestine and colon on day 7 are shown in Fig. S1 in the supplemental material.

We previously reported that *Tcf1* mutation does not affect the normal adult intestine (35). To determine the effects of the combined deletion of *Tcf1* and *Tcf3* in the colon and small intestine, we generated and analyzed Villin^{Creert2}_Tcf3$^{LoxP/LoxP}$_Tcf1^{Hom} compound mice (11, 23, 48). The intestine and the colon of these compound mice and their littermate controls were histologically analyzed at different days after *cre* induction (days 1, 3, 7, and 32). Intestinal sections were stained with cell-type-specific reagents to detect the differentiated cell types and proliferating cells. The Villin^{Creert2}_Tcf3$^{LoxP/LoxP}$_Tcf1^{Hom} mice exhibited, at all time points, normal numbers of stem, differentiated, and proliferating cells compared to their control littermates. The results of the histological analysis of the small intestine and colon on day 7 are shown in Fig. S1 in the supplemental material.

Thus, Tcf1 and/or Tcf3 appeared not to be critical for adult intestinal homeostasis.

Generation of a floxed *Tcf4* mouse. The murine *Tcf4* gene contains 17 exons, of which exons 10 and 11 encode the highly conserved DNA-binding domain of Tcf4. *Tcf4* homozygous KO animals die at about birth (23). To be able to study the consequence of *Tcf4* ablation in the adult intestine, we generated a *cre*-inducible floxed *Tcf4* mouse (see Fig. S2A in the supplemental material). In our KO construct, LoxP sites were placed around exon 11. This results in the functional inactivation of the Tcf4 protein and thereby the inactivation of Tcf4-mediated Wnt signaling, while the mutant mRNA and protein may still be expressed. The mouse *Tcf4* gene is subject to extensive alternative splicing (44, 49). To examine the presence of all known intestinal splice variants upon *cre* deletion, we reverse transcribed RNA from the intestines derived from two Villin^{Creert2}_Tcf4$^{LoxP/LoxP}$ mice and two control mice on day 5 after tamoxifen injection. *Tcf4*-specific sequences were PCR amplified with various combinations of exon-specific primer pairs (see Fig. S2B in the supplemental material) (49). This analysis showed the presence of all spice variants in the intestine upon the deletion of exon 11 (see Fig. S2B and C in the supplemental material). In addition, the presence of a major 231-bp band using specific primers surrounding the high mobility group (HMG) box demonstrated the efficient deletion of exon 10 in the intestine. Moreover, immunohistological staining showed the presence of wild-type (WT) Tcf4 protein (see Fig. S2D in the supplemental material) and mutant Tcf4 protein in the control and induced Villin^{Creert2}_Tcf4$^{LoxP/LoxP}$ mice, respectively (see Fig. S2E in the supplemental material).

To demonstrate that the deletion of the floxed *Tcf4* gene in mouse embryos yielded an identical phenotype in comparison with the classical *Tcf4*$^{hyg/hyg}$-KO mouse (23), we crossed the newly generated floxed *Tcf4* mouse with the PGK^{Cre} mouse. The PGK promoter drives *cre* expression in all cells, including the germ cells. The analysis of the intestine of PGK^{Cre}_Tcf4$^{Loxp/LoxP}$-KO embryos on day 17.5 days postcoitum (dpc) indeed revealed a phenotype identical to that of the classical *Tcf4*$^{hyg/hyg}$-KO mice, i.e., among others, the total absence of proliferative cells in the small intestinal crypt (Fig. 1C and D versus A and B) (23).

***Tcf4* is crucial for proliferation in the adult intestine.** To be able to study the consequence of specific ablation of *Tcf4* in the adult murine intestine, we generated Villin^{Creert2}_Tcf4$^{LoxP/LoxP}$ compound mouse. The colons of these mice and their littermate controls were analyzed on different days after *cre* induction (day 1 and 7). Deletion of *Tcf4* resulted in the regional absence of Ki67^{+} proliferating cells (Fig. 2B versus A). The detection of crypts with cycling Ki67^{+} cells within fields of Ki67^{-} cells probably represented crypts escaping deletion of the *Tcf4* gene (see arrows in Fig. 2B). Such escaper crypts are typically observed upon deletion of essential genes (30, 45). The combined data showed that Tcf4, in sharp contrast to Tcf1 and/or Tcf3, played an essential role in the homeostasis of the adult colon.

We next examined the small intestine of the

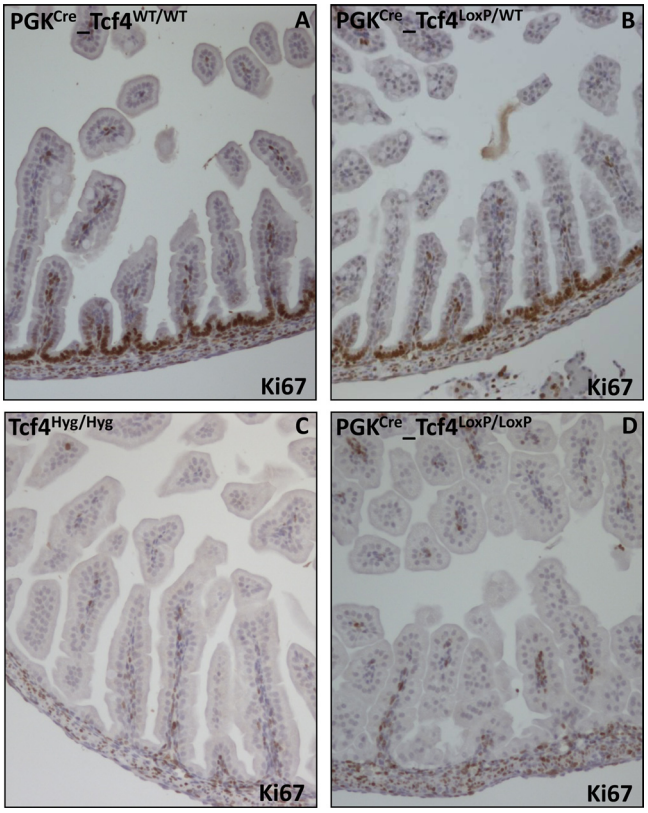

FIG 1 Absence of proliferating crypts in the small intestine derived from 17.5-dpc Tcf4$^{LoxP/LoxP}$_PGK^{Cre} mouse embryos. Histological analysis of the small intestine derived from 17.5-dpc mouse embryos showed the presence of proliferating/Ki67$^+$ cells in the control tissue derived from PGK^{Cre}_Tcf4$^{WT/WT}$ (A) and PGK^{Cre}_Tcf4$^{LoxP/WT}$ (B) mice, while the proliferating/Ki67$^+$ cells in the Tcf4$^{Hyg/Hyg}$ (C) and the PGK^{Cre}_Tcf4$^{LoxP/LoxP}$ (D) mice were completely abolished.

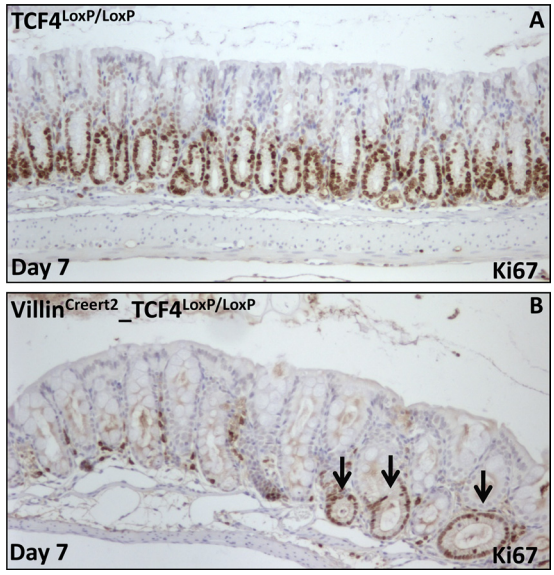

FIG 2 Lack of proliferating cells in the adult colon upon ablation of *Tcf4*. Histological analysis of the colon showed the presence of proliferating/Ki67$^+$ cells in the control tissue derived from Tcf4$^{LoxP/LoxP}$ mice (A) or Villin^{Creert2}_Tcf4$^{LoxP/LoxP}$ mice (data not shown), while the proliferating/Ki67$^+$ cells in the colon derived from the Villin^{Creert2}_Tcf4$^{LoxP/LoxP}$ mice (B) were abolished 7 days after *cre* induction.

Villin^{Creert2}_Tcf4$^{LoxP/LoxP}$ mice on different days after *cre* induction for the presence of proliferating cells. On day 1 after *cre* induction, normal numbers of Ki67$^+$ proliferating cells were present in the crypt of the Villin^{Creert2}_Tcf4$^{LoxP/LoxP}$ mice compared to littermate control mice (Fig. 3B versus A). However, on day 3 postinduction, the majority of the proliferating crypts were affected, while the remaining escaper crypts were in general still small, with limited numbers of proliferating cells (Fig. 3C). On day 7, proliferating crypts had almost entirely disappeared (Fig. 3D), with the exception of the hyperplastic escaper crypts. Such hyperplastic escaper crypts were absent in the proximal regions but increased in numbers more caudally, coinciding with reduced *cre* expression in these regions of the Villin^{Creert2} mice. The deletion of crypts coincided with the progressive loss of Wnt target gene expression such as CD44 and Sox9 (see Fig. S3 in the supplemental material). This dramatic phenotype was not compatible with life. At about day 9 after *cre* induction, the Villin^{Creert2}_Tcf4$^{LoxP/LoxP}$ mice had to be sacrificed due to the almost complete absence of intestinal crypt and villi in the small intestine.

These observations were confirmed in our recently developed intestinal organoid *in vitro* culture system (38). Under standard culture conditions, *cre* deletion of *Tcf4 in vitro* resulted in a complete block of Ki67$^+$ proliferating cells and subsequently the death of the organoid on day 6 (see Fig. S4 in the supplemental material).

We next examined the small intestine of the Villin^{Creert2}_Tcf4$^{LoxP/LoxP}$ mice for cell death via caspase 3 staining over a 7-day time course. On days 1 (see Fig. S5B in the supplemental material) and 2 (see Fig. S5D in the supplemental material) after *cre* induction, some caspase 3-positive (caspase 3$^+$) cells were present in the crypts of the Villin^{Creert2}_Tcf4$^{LoxP/LoxP}$ mice compared to littermate control mice (see Fig. S5A in the supplemental material). At 36 h postinduction, the majority of the crypts displayed apoptotic cells (see Fig. S5C in the supplemental material). From day 5 onwards, no caspase 3$^+$ cells could be detected (data not shown).

Stem cell niche in intestine of adult mice with *Tcf4* deletion. We subsequently analyzed the presence of intestinal stem cells by *in situ* hybridization. Olfm4 is a robust marker for intestinal Lgr5 stem cells (45, 46). On day 1 after *cre* induction, normal numbers of Olfm4$^+$ intestinal stem cells were present in the small intestine of the Villin^{Creert2}_Tcf4$^{LoxP/LoxP}$ (Fig. 3F versus E) compound mouse. However, on day 3 postinduction, the majority of the Olfm4$^+$ intestinal stem cells were eliminated (Fig. 3G). The small, remaining Ki67$^+$ proliferating escaper crypts did contain limited numbers of Olfm4$^+$ stem cells. On day 7, essentially all Olfm4$^+$ stem cells had disappeared (Fig. 3H). Olfm4$^+$ stem cells were, however, present in the escaper crypts (Fig. 3H, inset).

We next analyzed, using multiple-color single-molecule fluorescence *in situ* hybridization, the consequence of intestinal *Tcf4* inactivation on Lgr5 and Bmi1 expression. These proteins mark the intestinal stem cell and the presumed reserve pool of intestinal stem cells, respectively (2, 43). This analysis showed that the Wnt target, Lgr5, is present in the control and on day 1 upon *cre* activation (Fig. 4A and D and enlarged in Fig. 4B and E) but absent on day 3 (Fig. 4G; enlarged in Fig. 4H) and at later time points (results not shown) in the Villin^{Creert2}_Tcf4$^{LoxP/LoxP}$ mouse. These results were in sharp contrast with the expression pattern of *Bmi1*, itself not a Wnt target gene. *Bmi1* was expressed, as shown previously

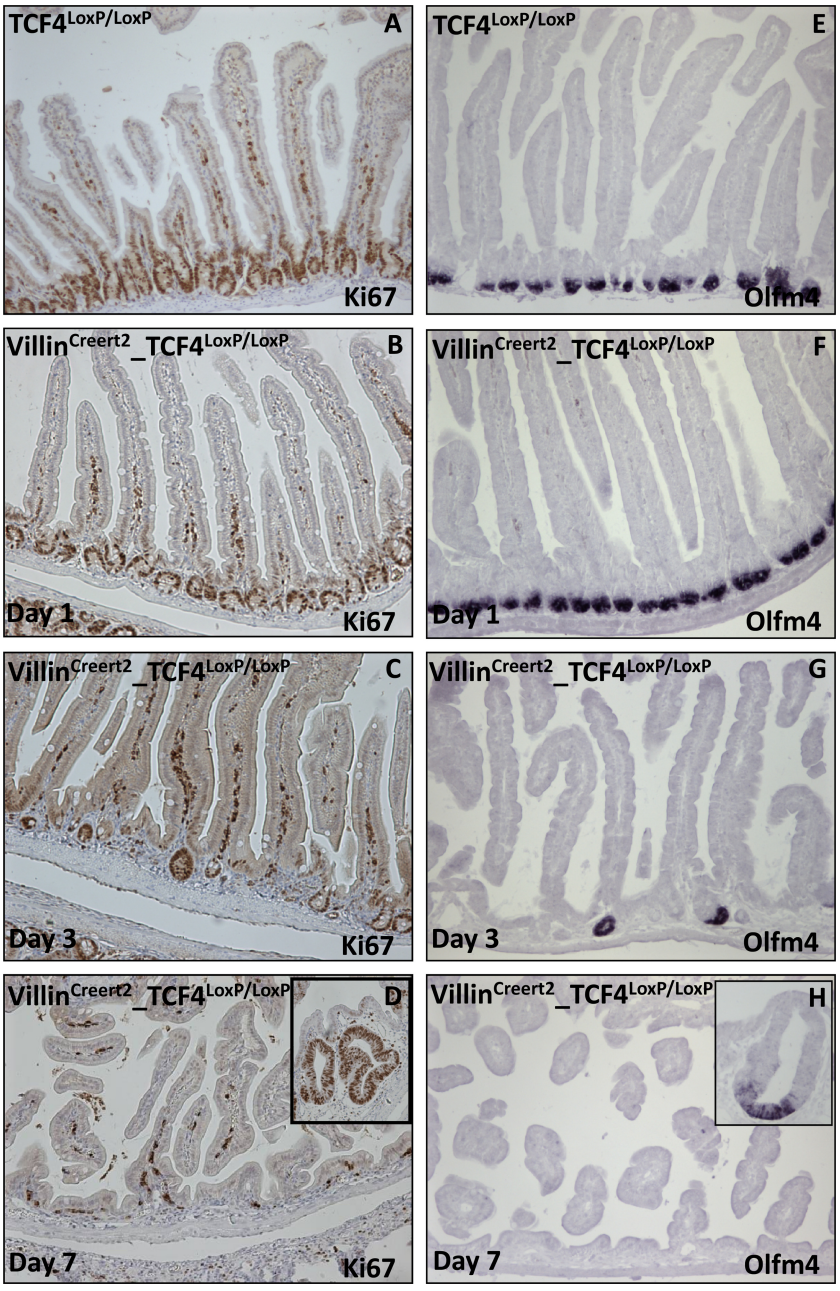

FIG 3 Lack of proliferating and stem cells in the adult small intestine upon ablation of *Tcf4*. Histological analysis at 1 day (B), 3 days (C), and 7 days (D) after tamoxifen-induced *cre* induction revealed, in comparison to a control $Tcf4^{LoxP/LoxP}$ mouse (A), the disappearance of proliferating/$Ki67^+$ cells over time in $Villin^{Creert2}$_$Tcf4^{LoxP/LoxP}$ mice. Occasionally, large hyperplastic, proliferative $Ki67^+$ escaper crypts (D, inset) could be detected. Histological analysis at 1 day (F), 3 days (G), and 7 days (H) after tamoxifen-induced *cre* induction revealed, in comparison to a control $Tcf4^{LoxP/LoxP}$ mouse (E), the disappearance of intestinal stem cell/$Olfm4^+$ cells over time in $Villin^{Creert2}$_$Tcf4^{LoxP/LoxP}$ mice. Occasionally, large hyperplastic, proliferative $Olfm4^+$ escaper crypts (H, inset) could be detected.

(19), throughout the intestinal crypt and was ultimately lost only when crypts had disappeared (Fig. 4A, D, and G, enlarged in Fig. 4B, E, and H, and results not shown). Therefore, the Wnt effector Tcf4 is required for the maintenance of the $Lgr5^+$ stem cells in the adult small intestine.

Recent *in vitro* and *in vivo* studies have shown that the direct neighbors of the $Lgr5^+$/$Olfm4^+$ intestinal stem cells, the Paneth cells, serve as an essential stem cell niche, providing Wnt, notch, and EGF signals (39). The Wnt signaling pathway is essential for terminal maturation of Paneth cells (47). Tcf4 is highly expressed in Paneth cells (47). The Wnt target gene, *EphB3*, encodes a sorting receptor that imposes downward migration of Paneth cells. In *EphB3*- and *frizzled-5*-knockout mice, Paneth cells no longer migrate to crypt bottoms but scatter along the crypt-villus axis (5, 47). This prompted us to investigate the presence and location of Paneth cells in the small intestine of the $Villin^{Creert2}$_$Tcf4^{LoxP/LoxP}$ mice on

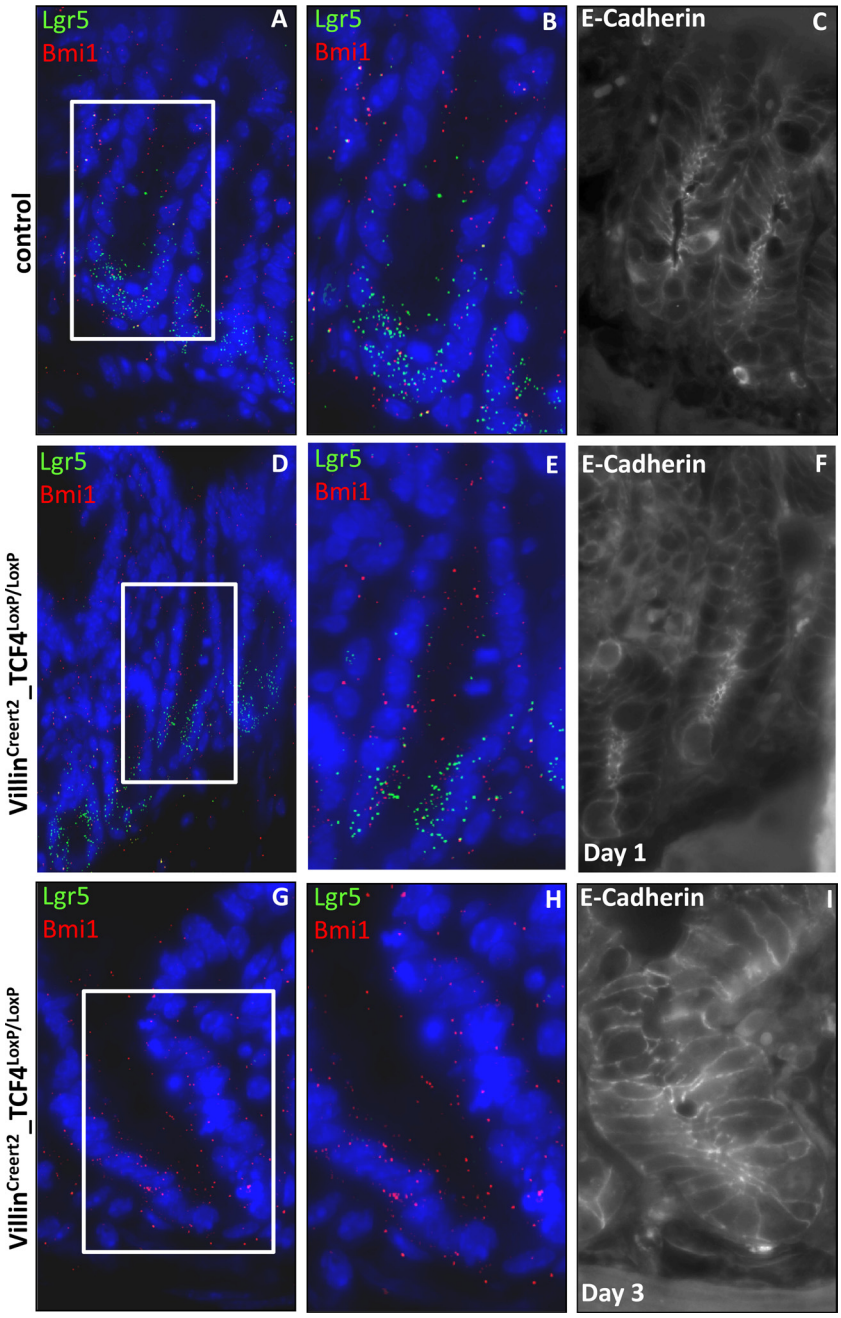

FIG 4 Lgr5 and Bmi1 expression in Tcf4-depleted crypt using two-color single-molecule fluorescent *in situ* hybridization. Tissue sections were simultaneously hybridized with two differentially labeled probe libraries (green, Lgr5-TMR; red, Bmi1-Cy5). Analysis at 1 day (D) and 3 days (G) after *cre* induction in the Villin^{Creert2}_Tcf4$^{LoxP/LoxP}$ mice revealed, in comparison to a control mouse (A), the disappearance of Lgr5^{+} cells over time, while Bmi1, scattered in the crypt, remained present. Magnification of representative areas is shown (B, E, and H). The E-cadherin stainings are used to show the cell borders (C, F, and I), while DAPI staining (A, D, and G) showed nuclear staining.

different days after *cre* induction. On day 1 after *cre* induction, normal numbers of lysozyme-positive Paneth cells were present in the small intestine of the induced Villin^{Creert2}_Tcf4$^{LoxP/LoxP}$ mice compared to their littermate controls (Fig. 5B versus A). However, on day 3 the majority of the lysozyme-positive Paneth cells were eliminated from the crypt of Lieberkühn and aberrantly located on the villi (Fig. 5C). The small remaining Ki67^{+} escaper crypts did contain limited numbers of correctly localized lysozyme-positive Paneth cells. On day 7 after *cre* induction, essentially all lysozyme-positive Paneth cells were eliminated (Fig. 5D). These dramatic observations were confirmed by *in situ* hybridization with the Paneth cell-specific cryptdin-1 as the probe (Fig. 5E to H). Moreover, these data also suggested that on day 3 after *cre* induction, some goblet cells expressed the Paneth cell marker cryptdin-1. These features are consistent with previous descriptions of the rare so-called intermediate cells, which are considered to be in transition between undifferentiated cells and Paneth and

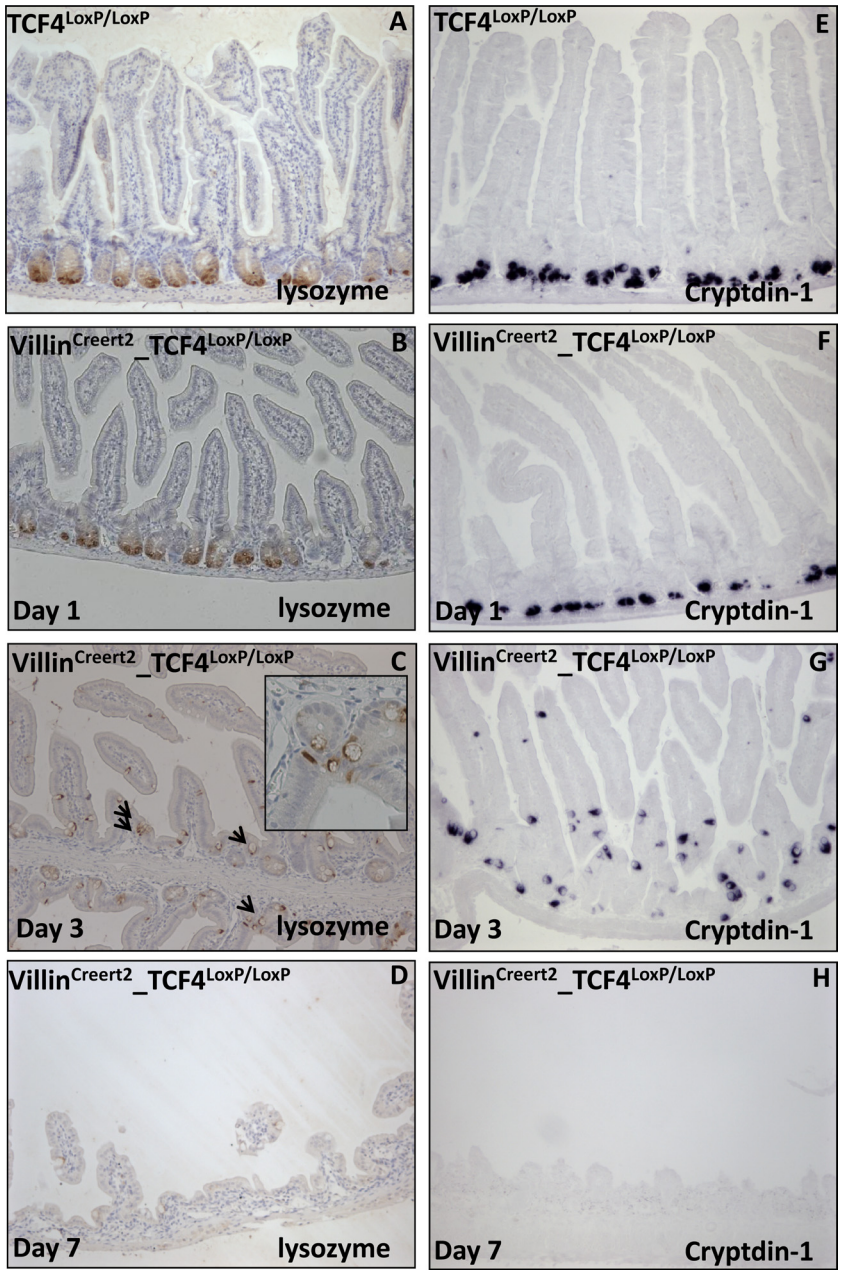

FIG 5 Lack of crypt-based Paneth cells in the adult small intestine upon ablation of *Tcf4*. Histological analysis via lysozyme staining at 1 day (B), 3 days (C), and 7 days (D) after *cre* induction revealed, in comparison to a control mouse (A), the elimination of Paneth cells from the crypt of Lieberkühn and the aberrant location of these Paneth cells on the villi (see arrows in panel C and a magnified view in the inset). *In situ* hybridization analysis using cryptdin-1 as probe at 1 day (F), 3 days (G), and 7 days (H) after *cre* induction revealed, in comparison to a control mouse (E), the disappearance of cryptdin-1$^+$ Paneth cells at the bottom of the crypt of Lieberkühn over time. At day 3, cryptdin-1$^+$ cells Paneth and non-Paneth (intermediate) cells are scattered through the crypt and villi.

goblet cells (6). Indeed, histological double staining revealed the presence of large numbers of PAS$^+$/cryptdin-1$^+$ goblet-like cells in the intestine derived from Villin^{Creert2}_Tcf4$^{LoxP/LoxP}$ mice on day 3 after *cre* induction; goblet-like cells were absent in the intestine derived from the control mice (Fig. 6B versus A). Moreover, cryptdin-1 double-labeling studies showed that cryptdin-1$^+$ cells could never be detected in combination with the other secretory cell types such as enteroendocrine cells (Fig. 6D versus C) or tuft cells (Fig. 6F versus E).

Therefore, the loss of cell proliferation and stem cells in the intestinal crypts of tamoxifen-induced Villin^{Creert2}_Tcf4$^{LoxP/LoxP}$ coincides with the depletion and aberrant migration of Paneth (precursor) cells.

The outcome of the histological analysis of the Tcf4 mutant intestine was further confirmed by electron microscopy (EM) analysis. EM analysis on day 1 postinduction showed the release of granules by Paneth cells and the first sign of decline of the intestinal stem cells (Fig. 7C and D). On day 3, missorted Paneth cells, Paneth cells with very small or electron-lucent granules, and the decline of stem cells were clearly visible (Fig. 7E and F). On day 6 after *cre* induction, irregular nonorganized crypts, the absence of

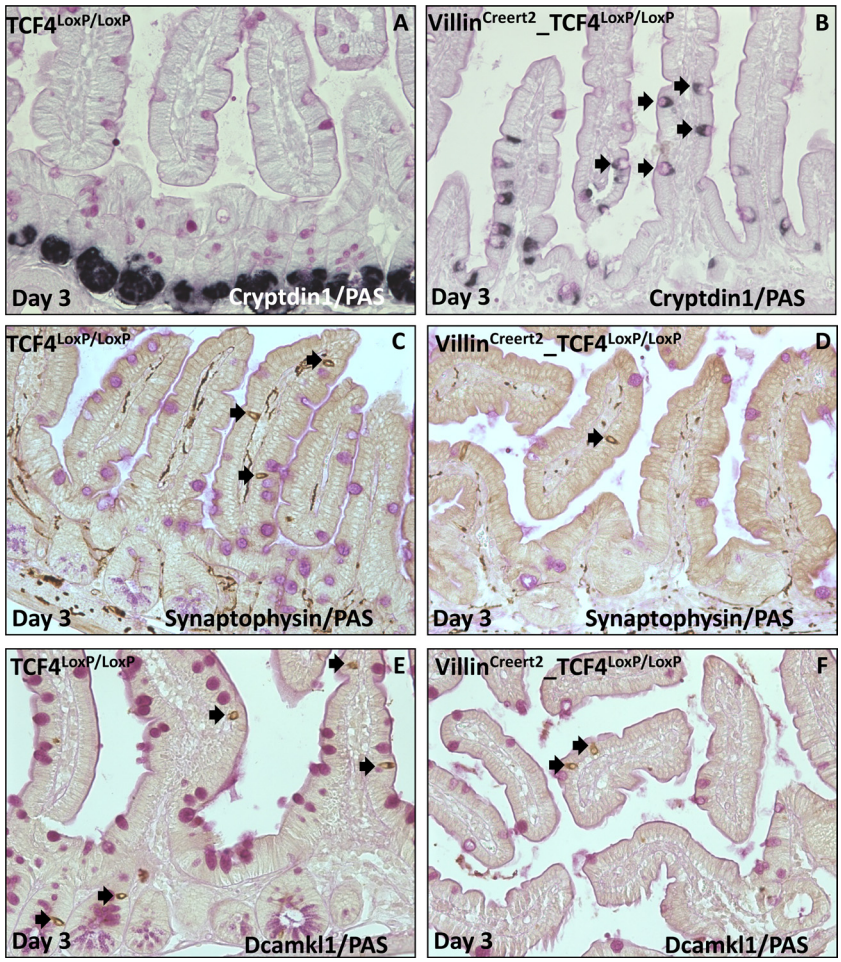

FIG 6 Generation of large numbers of intermediate cells upon *Tcf4* ablation. Histological double staining showed generation of PAS^+/cryptdin-1^+ intermediate cells in the intestine in the $Villin^{Creert2}$_$Tcf4^{LoxP/LoxP}$ mice on day 3 after *cre* induction (panel B versus A, arrows). cryptdin-1^+ cells could never be detected in combination with enteroendocrine cells (D versus C, arrows) or tuft cells (panel F versus E, arrows).

Paneth and stem cells, and the presence of undifferentiated TA-like cells could be detected (Fig. 7G and H).

Of note, simultaneous deletion of *Tcf1*, *Tcf3*, and *Tcf4* in the small or large intestine using the compound $Villin^{Creert2}$_$Tcf4^{LoxP/LoxP}$_$Tcf3^{LoxP/LoxP}$_$Tcf1^{hom}$ mice revealed no additional histological changes in the phenotype in comparison to that with the ablation of *Tcf4* alone (results not shown).

DISCUSSION

The Wnt genetic program is activated upon a nuclear interaction of β-catenin with a member of the TCF family (Tcf1, Lef, Tcf3, and Tcf4). Determination of the individual roles of the different members of the TCF family in vertebrate Wnt signaling is complicated by the redundancy of these transcription factors. Indeed, they are expressed in distinct but overlapping patterns in the developing mouse embryo and in adult tissue such as skin and intestine (15, 31).

In embryonic skin, Tcf3, Tcf4, and Lef1 are expressed in basal progenitors. As morphogenesis proceeds, the expression of Lef1 (base of the growing hair follicle) and Tcf3/4 (hair follicle stem cells) diverges (31). In adult mice, skin-specific conditional ablation of *Tcf3* or *Tcf4* shows no deleterious impact on epithelial homeostasis. However, the *Tcf3/4*-null mice showed early defects in epidermal stability and hair follicle morphogenesis. In addition, hair reconstitution and wound repair assays showed that the *in vivo* regenerative capacity of *Tcf3/4*-null adult epithelial stem cells was severely compromised, while *in vitro Tcf3/4*-null epithelial stem cells lost the ability to self-renew in culture. Collectively, this study shows that the skin epithelial stem cells are severely crippled in the combined absence of both *Tcf3* and *Tcf4*.

In the embryonic intestine, the analysis of *Tcf4/Tcf1* double-null mice showed that at early embryonic stages, the Wnt signaling pathway regulates the expansion and patterning of the gastrointestinal tract (15). While *Tcf1*-null mice do not show an intestinal phenotype in neonatal and adult mice, the phenotype of the $Tcf4^{hyg}$-null mice first becomes evident at about E16.5 as a lack of the establishment of crypt stem cell compartments (23).

The role of most of these Wnt effectors in the homeostasis of the adult mouse intestinal epithelium was previously unresolved. Via the specific inactivation of the different downstream effectors of the Wnt signaling pathway (Tcf1, Tcf3, and Tcf4) in the intestine, we now demonstrate that Tcf4 is the key player in these cellular processes, while the other members are surprisingly dispensable.

Angus-Hill et al. (1) have recently shown hyperproliferation in

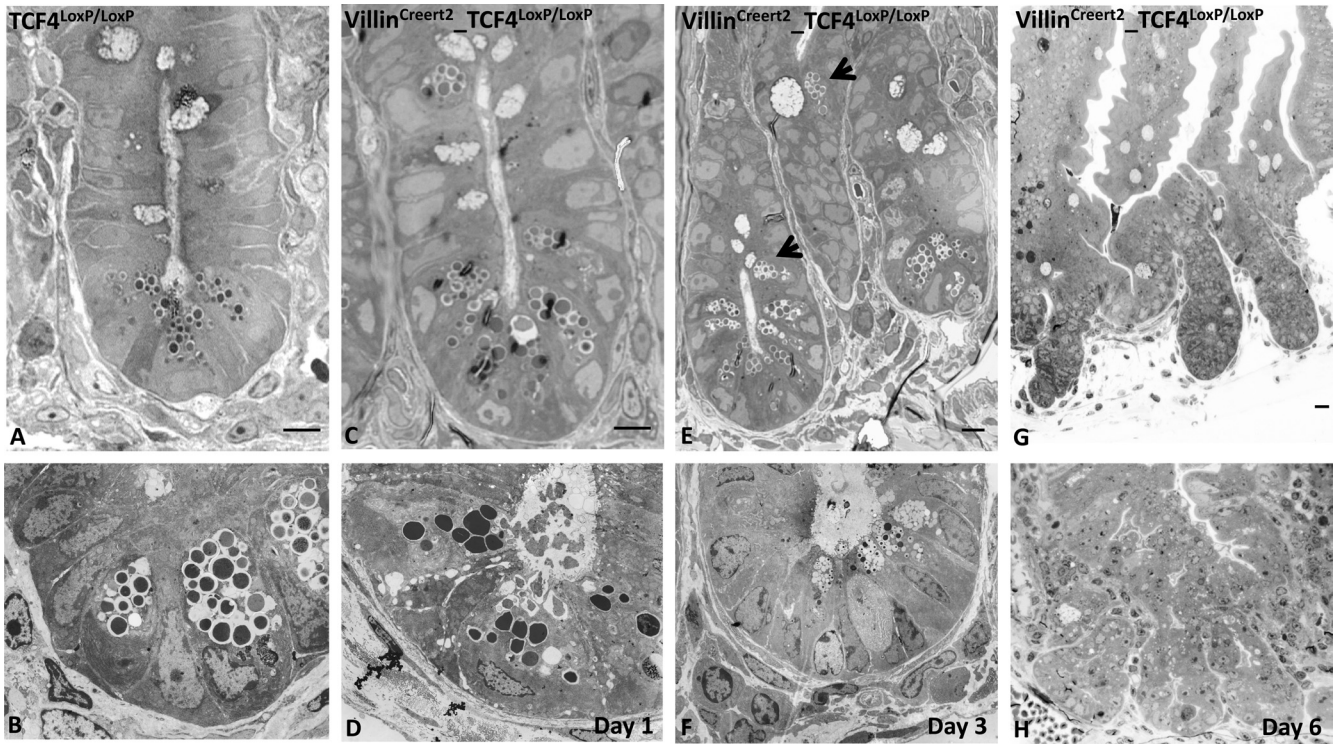

FIG 7 EM analysis of *Tcf4*-ablated small intestines. EM analysis of Tcf4-depleted intestine derived from the Villin^{Creert2}_Tcf4$^{LoxP/LoxP}$ mice at 1 day (C and D), 3 days (E and F), and 7 days (G and H) after *cre* induction revealed the gradual disappearance of intestinal stem cells, Paneth cells, and, ultimately, the complete proliferating crypt. Arrows indicate escaping Paneth cells on day 3 after *cre* induction (E). Bar, 10 μm.

the adult colon upon *Tcf4* ablation but did not analyze the small intestine. The authors concluded that Tcf4 acts as a tumor suppressor since haploinsufficiency resulted in increased tumor formation in the colon of APCmin mice but, somewhat surprisingly, not in the small intestine. The apparent disparity with the current observations might be due to differences between the floxed alleles. Our floxed *Tcf4* mice, upon *cre* deletion, produced a non-DNA-binding version of Tcf4, while the allele of Angus-Hill et al. deletes the ATG-containing exon 1 (1). In addition, we have used the well-characterized inducible intestine-specific *cre* line (Villin^{Creert2}), which is also active in intestinal stem cells, while Angus-Hill et al. have applied a constitutive *Tcf4*^{Cre} mouse (1).

In conclusion, we demonstrated here an essential role for Tcf4 during homeostasis of the adult mouse intestinal tract. The newly generated floxed *Tcf4* allele may be instrumental to study the role of Tcf4 in (intestinal) tumorigenesis and diabetes (14).

ACKNOWLEDGMENTS

We thank E. Fuchs for providing the floxed *Tcf3* mice.

This research was supported by grants from TI Pharma (to J.H.V.E. and M.V.D.B.), KWF (to P.K.), NWO-Spinoza (to A.H.), the European Molecular Biology Organization (to A.H.), ERC 232814 (to S.F.B.), and the Maag-Lever-Darm Stichting (to A.H.).

We declare no competing financial interests.

REFERENCES

1. **Angus-Hill ML, Elbert KM, Hidalgo J, Capecchi MR.** 2011. T-cell factor 4 functions as a tumor suppressor whose disruption modulates colon cell proliferation and tumorigenesis. Proc. Natl. Acad. Sci. U. S. A. **108**:4914–4919.
2. **Barker N, et al.** 2007. Identification of stem cells in small intestine and colon by marker gene Lgr5. Nature **449**:1003–1007.
3. **Bass AJ, et al.** 2011. Genomic sequencing of colorectal adenocarcinomas identifies a recurrent *VTI1A-TCF7L2* fusion. Nat. Genet. **43**:964–968.
4. **Bastide P, et al.** 2007. Sox9 regulates cell proliferation and is required for Paneth cell differentiation in the intestinal epithelium. J. Cell Biol. **178**:635–648.
5. **Batlle E, et al.** 2002. Beta-catenin and TCF mediate cell positioning in the intestinal epithelium by controlling the expression of EphB/ephrinB. Cell **111**:251–263.
6. **Calvert R, Bordeleau G, Grondin G, Vezina A, Ferrari J.** 1988. On the presence of intermediate cells in the small intestine. Anat. Rec. **220**:291–295.
7. **Cheng H, Leblond CP.** 1974. Origin, differentiation and renewal of the four main epithelial cell types in the mouse small intestine. V. Unitarian theory of the origin of the four epithelial cell types. Am. J. Anat. **141**:537–561.
8. **Cheng H, Leblond CP.** 1974. Origin, differentiation and renewal of the four main epithelial cell types in the mouse small intestine. I. Columnar cell. Am. J. Anat. **141**:461–479.
9. **Chien AJ, Conrad WH, Moon RT.** 2009. A Wnt survival guide: from flies to human disease. J. Investig. Dermatol. **129**:1614–1627.
10. **de Lau W, et al.** 2011. Lgr5 homologues associate with Wnt receptors and mediate R-spondin signalling. Nature **476**:293–297.
11. **el Marjou F, et al.** 2004. Tissue-specific and inducible Cre-mediated recombination in the gut epithelium. Genesis **39**:186–193.
12. **Escobar M, et al.** 2011. Intestinal epithelial stem cells do not protect their genome by asymmetric chromosome segregation. Nat. Commun. **2**:258.
13. **Gerbe F, et al.** 2011. Distinct ATOH1 and Neurog3 requirements define tuft cells as a new secretory cell type in the intestinal epithelium. J. Cell Biol. **192**:767–780.
14. **Grant SF, et al.** 2006. Variant of transcription factor 7-like 2 (TCF7L2) gene confers risk of type 2 diabetes. Nat. Genet. **38**:320–323.
15. **Gregorieff A, Grosschedl R, Clevers H.** 2004. Hindgut defects and trans-

formation of the gastro-intestinal tract in Tcf4($^{-/-}$)/Tcf1($^{-/-}$) embryos. EMBO J. **23**:1825–1833.
16. **Gregorieff A, et al.** 2005. Expression pattern of Wnt signaling components in the adult intestine. Gastroenterology **129**:626–638.
17. **Hazra A, Fuchs CS, Chan AT, Giovannucci EL, Hunter DJ.** 2008. Association of the TCF7L2 polymorphism with colorectal cancer and adenoma risk. Cancer Causes Control **19**:975–980.
18. **Ireland H, et al.** 2004. Inducible Cre-mediated control of gene expression in the murine gastrointestinal tract: effect of loss of beta-catenin. Gastroenterology **126**:1236–1246.
19. **Itzkovitz S, et al.** 2011. Single-molecule transcript counting of stem-cell markers in the mouse intestine. Nat. Cell Biol. **14**:106–114.
20. **Kim CH, et al.** 2000. Repressor activity of Headless/Tcf3 is essential for vertebrate head formation. Nature **407**:913–916.
21. **Kim KA, et al.** 2005. Mitogenic influence of human R-spondin1 on the intestinal epithelium. Science **309**:1256–1259.
22. **Korinek V, et al.** 1997. Constitutive transcriptional activation by a beta-catenin-Tcf complex in APC$^{-/-}$ colon carcinoma. Science **275**:1784–1787.
23. **Korinek V, et al.** 1998. Depletion of epithelial stem-cell compartments in the small intestine of mice lacking Tcf-4. Nat. Genet. **4**:379–383.
24. **Kuhnert F, et al.** 2004. Essential requirement for Wnt signaling in proliferation of adult small intestine and colon revealed by adenoviral expression of Dickkopf-1. Proc. Natl. Acad. Sci. U. S. A. **101**:266–271.
25. **Liu W, et al.** 2000. Mutations in AXIN2 cause colorectal cancer with defective mismatch repair by activating beta-catenin/TCF signalling. Nat. Genet. **26**:146–147.
26. **Marshman E, Booth C, Potten CS.** 2002. The intestinal epithelial stem cell. Bioessays **24**:91–98.
27. **Merrill BJ, Pasolli et al.** 2004. Tcf3: a transcriptional regulator of axis induction in the early embryo. Development **131**:263–274.
28. **Mori-Akiyama Y, et al.** 2007. SOX9 is required for the differentiation of Paneth cells in the intestinal epithelium. Gastroenterology **133**:539–546.
29. **Morin PJ, et al.** 1997. Activation of beta-catenin-Tcf signaling in colon cancer by mutations in beta-catenin or APC. Science **275**:1787–1790.
30. **Muncan V, et al.** 2006. Rapid loss of intestinal crypts upon conditional deletion of the Wnt/Tcf-4 target gene c-Myc. Mol. Cell. Biol. **26**:8418–8426.
31. **Nguyen H, et al.** 2009. Tcf3 and Tcf4 are essential for long-term homeostasis of skin epithelia. Nat. Genet. **41**:1068–1075.
32. **Nishisho I, et al.** 1991. Mutations of chromosome 5q21 genes in FAP and colorectal cancer patients. Science **253**:665–669.
33. **Párrizas M, et al.** 2001. Hepatic nuclear factor 1-alpha directs nucleosomal hyperacetylation to its tissue-specific transcriptional targets. Mol. Cell. Biol. **21**:3234–3243.
34. **Pinto D, Gregorieff A, Begthel H, Clevers H.** 2003. Canonical Wnt signals are essential for homeostasis of the intestinal epithelium. Genes Dev. **17**:1709–1713.
35. **Roose J, et al.** 1999. Synergy between tumor suppressor APC and the beta-catenin-Tcf4 target Tcf1. Science **285**:1923–1926.
36. **Sangiorgi E, Capecchi MR.** 2008. Bmi1 is expressed *in vivo* in intestinal stem cells. Nat. Genet. **40**:915–920.
37. **Sansom OJ, et al.** 2004. Loss of Apc in vivo immediately perturbs Wnt signaling, differentiation, and migration. Genes Dev. **18**:1385–1390.
38. **Sato T, et al.** 2009. Single Lgr5 stem cells build crypt-villus structures in vitro without a mesenchymal niche. Nature **459**:262–265.
39. **Sato T, et al.** 2011. Paneth cells constitute the niche for Lgr5 stem cells in intestinal crypts. Nature **469**:415–418.
40. **Schepers AG, Vries R, van den Born M, van de Wetering M, Clevers H.** 2011. Lgr5 intestinal stem cells have high telomerase activity and randomly segregate their chromosomes. EMBO J. **30**:1104–1109.
41. **Slattery ML, et al.** 2008. Transcription factor 7-like 2 polymorphism and colon cancer. Cancer Epidemiol. Biomarkers Prev. **17**:978–982.
42. **Snippert HJ, et al.** 2010. Intestinal crypt homeostasis results from neutral competition between symmetrically dividing Lgr5 stem cells. Cell **143**:134–144.
43. **Tian H, et al.** 2011. A reserve stem cell population in small intestine renders Lgr5-positive cells dispensable. Nature **478**:255–259.
44. **Vacik, T, Stubbs JL, Lemke G.** 2011. A novel mechanism for the transcriptional regulation of Wnt signaling in development. Genes Dev. **25**:1783–1795.
45. **van der Flier LG, et al.** 2009. Transcription factor achaete scute-like 2 controls intestinal stem cell fate. Cell **136**:903–912.
46. **van der Flier LG, Haegebarth A, Stange DE, van DE Wetering M, Clevers H.** 2009. OLFM4 is a robust marker for stem cells in human intestine and marks a subset of colorectal cancer cells. Gastroenterology **137**:15–17.
47. **van Es JH, et al.** 2005. Wnt signalling induces maturation of Paneth cells in intestinal crypts. Nat. Cell Biol. **7**:381–386.
48. **Verbeek S, et al.** 1995. An HMG-box-containing T-cell factor required for thymocyte differentiation. Nature **374**:70–73.
49. **Weise A, et al.** 2010. Alternative splicing of Tcf7l2 transcripts generates protein variants with differential promoter-binding and transcriptional activation properties at Wnt/beta-catenin targets. Nucleic Acids Res. **38**:1964–1981.
50. **Wend P, Holland JD, Ziebold U, Birchmeier W.** 2010. Wnt signaling in stem and cancer stem cells. Semin. Cell Dev. Biol. **21**:855–863.